AIP | Applied Physics Letters

Electric field and temperature-induced phase transition in Mn-doped Na1/2Bi1/2TiO3-5.0 at.%BaTiO3 single crystals investigated by micro-Raman scattering

Chao Chen, Haiwu Zhang, Hao Deng, Ting Huang, Xiaobing Li, Xiangyong Zhao, Zhigao Hu, Dong Wang, and Haosu Luo

Citation: Applied Physics Letters **104**, 142902 (2014); doi: 10.1063/1.4870504
View online: http://dx.doi.org/10.1063/1.4870504
View Table of Contents: http://scitation.aip.org/content/aip/journal/apl/104/14?ver=pdfcov
Published by the AIP Publishing

Electric field and temperature-induced phase transition in Mn-doped $Na_{1/2}Bi_{1/2}TiO_3$-5.0 at.%$BaTiO_3$ single crystals investigated by micro-Raman scattering

Chao Chen,[1,2,3,a)] Haiwu Zhang,[1,3] Hao Deng,[1,3] Ting Huang,[4] Xiaobing Li,[1] Xiangyong Zhao,[1] Zhigao Hu,[4] Dong Wang,[1] and Haosu Luo[1,a)]
[1]*Key Laboratory of Inorganic Functional Materials and Devices, Shanghai Institute of Ceramics, University of Chinese Academy of Sciences, 215 Chengbei Road, Jiading, Shanghai 201800, China*
[2]*Department of Materials Science and Engineering, Jiangxi Key Laboratory of Advanced Ceramic Materials, Jingdezhen Ceramic Institute, Jingdezhen 333001, China*
[3]*University of Chinese Academy of Sciences, Beijing 100049, China*
[4]*Department of Electronic Engineering, East China Normal University, Shanghai 200241, People's Republic of China*

(Received 7 January 2014; accepted 23 March 2014; published online 7 April 2014)

A micro-Raman scattering technique was used to investigate the electric-field and temperature dependent phase stability of Mn-doped $Na_{1/2}Bi_{1/2}TiO_3$-5.0at.%$BaTiO_3$ single crystal. The Ti–O mode was found to exhibit a slight shift at a low electric field ($E = 10\,kV/cm$) and splitting at higher electric field ($E \geq 30\,kV/cm$), ascribed to field-induced local distortion and phase transition, respectively. The temperature-dependent Raman scattering was also measured over a wide range of 150–800 K to study the phase stability of poled samples. A new Raman mode at about $200\,cm^{-1}$ and an anomaly in intensity of the Ti-O modes were detected at 390 K, indicating a ferroelectric to antiferroelectric phase transition. The frequency shift of TiO_6 octahedral modes implied a transition to a paraelectric state at 550 K. Furthermore, the Ti-O and TiO_6 octahedral modes were found to be sustained in the high-temperature paraelectric state. © *2014 AIP Publishing LLC*. [http://dx.doi.org/10.1063/1.4870504]

Extensive study of the $(1-x)Na_{1/2}Bi_{1/2}TiO_3$-$xBaTiO_3$ (NBT-x%BT) piezoelectric system has demonstrated the potential of these materials as lead-free alternatives to lead zirconate titanate (PZT). The system contains a morphotropic phase boundary (MPB) between the rhombohedral (R) and tetragonal (T) structures near $6.0 < x < 8.0$,[1,2] where these compositions possess intriguing structural and electrical properties. In particular, longitudinal piezoelectric d_{33} coefficients as high as 480 pC/N have been reported for Mn-doped NBT-5.6%BT single crystals after poling along the [001] direction.[3]

To clarify the origin of the strong piezoelectric response in the vicinity of the MPB region, the evolution of phase structure with electric (E)-field has been extensively investigated using X-ray diffraction (XRD) and transmission electron microscopy (TEM). Based on the splitting of the pseudocubic (200) reflection of NBT-x%BT ($5.0 < x < 7.0$), Ge *et al*. and Daniels *et al*. proposed that an E-field induced phase transformation from pseudocubic to T structure is responsible for the large electrically induced strain.[4,5] TEM images[6] of $x = 6.0$ ceramics have shown the coexistence of $R3c$ and $P4bm$ polar nanoregions (or nanodomains) at room temperature. Electric-field *in situ* TEM[7] has revealed that the overall poling-induced phase transitions in these $x = 6.0$ ceramics can be described as $R3c/P4bm \rightarrow R3c \rightarrow P4mm/R3c$. This finding implies that the piezoelectric enhancement may be ascribed to the development of the polar nanoregions, allowing the existence of lower energy barriers for dipole reorientation/switching under an external E-field.[7]

On the other hand, the structural modifications induced by an E-field significantly depend on the thermal history near the MPB.[8–10] Previous dielectric investigations have shown that an E-field induced ferroelectric state transforms into a relaxor state on heating around the depolarization temperature (T_d).[8] Most importantly, the piezoelectric properties exhibited an abrupt decrease at this point, possibly due to the change in the distribution of bonds parallel to $[001]_c$, e.g., the nucleation of $P4bm$ nanodomains.[9] In fact, hot stage TEM on $x = 6.0$ ceramics has revealed that P4bm nanodomains start to grow in volume above T_d, and gradually evolve into $Pm3m$ cubic structure on further heating.[10] However, XRD measurements on $5.0 < x < 7.0$ samples revealed no apparent distortions at any temperature, indicating no structural transformation.[11]

Raman spectroscopy provides another useful probe to investigate local structure and phase transition in relaxor-based ferroelectrics.[12–18] Kreisel *et al*. carried out high-pressure Raman measurements on NBT and proposed a pressure-induced relaxor-to-antiferroelectric crossover.[13] Recently, temperature-dependent Raman studies of NBT-x%BT materials have also been reported.[14,15] However, Raman studies as a function of poling E-field have not yet been presented. Interestingly, Shen *et al*. detected a unique mode upon heating [001]-poled $0.67Pb(Mg_{1/3}Nb_{2/3})O_3$–$0.33PbTiO_3$ single crystal that signified the relaxor to ferroelectric phase transition.[12] Whether a similar variation exists for NBT-x%BT single crystals near the MPB composition is still unknown, especially across T_d, where the materials exhibit relaxor behavior.[6,8]

In this letter, we report a Raman investigation on Mn-doped NBT-5.0%BT (Mn: NBT-5.0%BT) single crystal, which is located around the MPB with a slight amount of Mn

a)Author to whom correspondence should be addressed. Electronic mail: hsluo@mail.sic.ac.cn and cc2762@163.com.

introduced to improve the poling process. Raman spectra were measured for [001]-oriented samples under different poling *E*-fields. The application of an *E*-field was found to align the randomly distributed nanodomains along the external *E*-field direction, followed by a transition from *R* to *T* phase. Temperature-dependent Raman studies were also performed on a [001]-poled sample. A unique Raman mode at $\sim 200\,cm^{-1}$ was found around T_d, signifying a ferroelectric to relaxor phase transition. These findings have implications to additional NBT-*x*%BT composition and other relaxor ferroelectrics.

Single crystals of Mn:NBT-*x*%BT were grown by a top-seeded solution growth method. The concentrations of Ba and Mn ions in the crystals were determined to be 5.0 and 0.14 at. %, respectively, by inductively coupled plasma atomic emission spectrometry (ICP-AES). The [001]-oriented Mn:NBT-5.0at. %BT crystal wafers with dimensions of $4 \times 4 \times 0.4\,mm^3$ were cut from the boule, and electroded on both (100) faces with gold. The samples were poled under different dc *E*-fields of 10 kV/cm, 20 kV/cm, 30 kV/cm, and 40 kV/cm at 350 K in silicon oil bath. The piezoelectric constant (d_{33}) was measured by a quasi-static Berlincourt type meter of ZJ-3A type. Then the samples were carefully polished for Raman scattering studies. Temperature dependent Raman scattering experiments were carried out using a Jobin-Yvon LabRAM HR 800 UV micro-Raman spectrometer equipped with a Linkam THMSE 600 heating stage from 150 to 800 K.

Although previous Raman studies[13–18] on NBT-based materials have shown that the number of detectable Raman modes is less than that predicted theoretically, these modes can be divided into three main regions: (1) a low wavenumber range of 100–200 cm^{-1} assignable to the vibrations of *A* site cations; (2) a middle wavenumber range of 200–400 cm^{-1} related to the vibrations of Ti-O bond; (3) a high wavenumber range of 450–650 cm^{-1} associated with the vibrations of TiO_6-octahedra.

The Raman spectra of [001]-oriented Mn:NBT-5.0%BT crystals under different poling *E*-fields are shown in Fig. 1(a). The spectrum of the unpoled sample (Fig. 1(b)) displayed a Ti-O peak centered at 293 cm^{-1} and a triplet splitting of oxygen octahedral vibrational modes located at 497 cm^{-1}, 554 cm^{-1}, and 618 cm^{-1}, respectively. Similar peaks were clearly observed in the Raman spectra of NBT-5.0%BT,[15,18] indicating that the composition present was located on the *R* side of the MPB region. At a poling *E*-field of 10 kV/cm, the Raman peaks displayed no obvious changes except a slight redshift of the Ti-O mode (293 cm^{-1}). This may be ascribed to local distortions instead of phase transformation. Slodczyk *et al.* stated that Ti–O bonds are influenced by nanodomain dynamics.[19] Additionally, such nanodomains are considered to be nonequilibrium states that are greatly affected by external conditions (i.e., *E*-field and temperature).[6,7] Thus, it can be understood that the polar nanodomains were substantially oriented compared with those in the unpoled case, resulting in enhanced local ordering. A similar phenomenon has also been observed for a lead-based relaxor ferroelectric.[20] The Ti-O peak became broader when the *E*-field was further increased to 20 kV/cm (Fig. 1(a)). Notable changes were

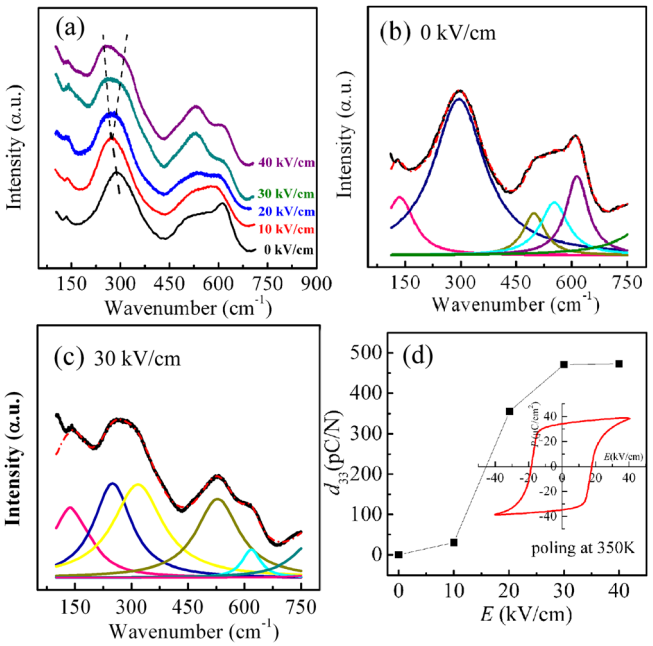

FIG. 1. Raman spectra for various poling E-field (a) and deconvolution of Raman spectra for (b) 0 kV/cm and (c) 30 kV/cm, and the piezoelectric constant (d_{33}) as a function of poling E-field (d) for [001]-oriented Mn:NBT-5.0%BT crystals.

observed at 30 kV/cm, as shown in Fig. 1(c). The single Ti–O mode split into two peaks (249 cm^{-1} and 315 cm^{-1}), indicating a typical of tetragonal symmetry. Meanwhile, the mode at 497 cm^{-1} merged into the mode at 554 cm^{-1} and made the three Raman modes observed at lower *E*-field become two (526 cm^{-1} and 618 cm^{-1}). It is believed that these changes were caused by irreversible *E*-field driven *R* to *T* phase transition. It should be noted that these electric-field-dependent spectra are quite similar to the NBT-*x*%BT Raman spectra observed during the *R* (*R*3c) to *T* (*P*4mm) phase transition induced by BT content.[15,18]

The corresponding longitudinal piezoelectric coefficient (d_{33}) of the samples under different poling *E*-fields are also shown in Fig. 1(d). The d_{33} begins to appear at 10 kV/cm. This low *E*-field aligned the randomly oriented nanodomains along the direction of the *E*-field, resulting in enhanced local ordering. The d_{33} exhibited an abrupt change at 20 kV/cm, which is close to the coercive field ($\sim$20 kV/cm) of the samples at its poling temperature (350 K) [determined from the polarization loop shown in the inset of Fig. 1(d)]. This suggests that the energy cost of the *R*-*T* transformation is somewhat comparable to the energy needed to trigger the formation of long-ranged ordered ferroelectric macrodomains. Above 30 kV/cm, the d_{33} became saturated at a higher level. Therefore, it is confirmed that the highest d_{33} occurred in the *T* phase side of the MPB after poling, which is in good agreement with previously reported XRD data.[21]

Figure 2 shows temperature dependent Raman spectra for [001]-poled samples (at 30 kV/cm) with different thermal history: (a) zero field heating (ZFH) and (b) zero field cooling (ZFC). The frequencies, bandwidths, and intensities of the peaks in the Raman spectra for the ZFH condition were essentially temperature independent in the temperature range 150–375 K (Fig. 2(a)). This invariable condition means that

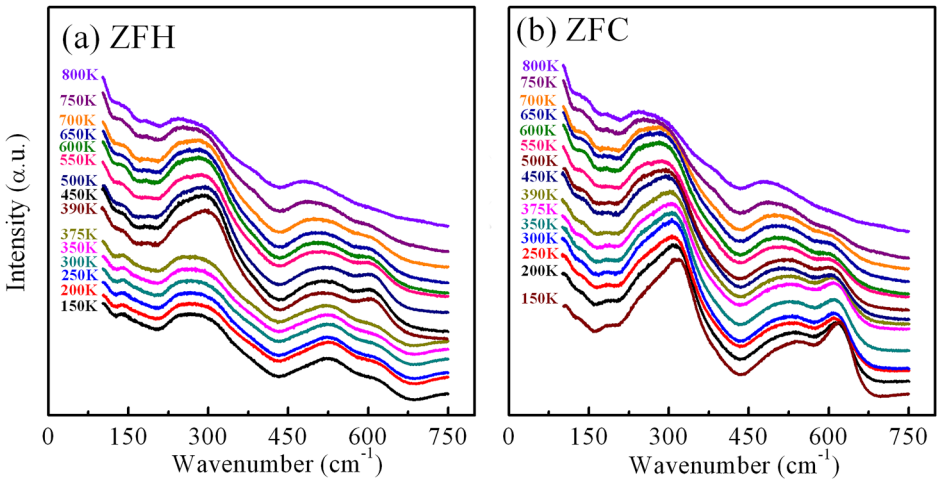

FIG. 2. Raman spectra for [001]-poled Mn:NBT-5.0%BT crystals during different thermal history: (a) ZFH; (b)ZFC.

the *E*-field induced *T* ferroelectric state was stable upon heating to 375 K. When the temperature was further increased to 390 K, anomalies in the peak numbers, bandwidths, and mode intensities were observed. To better illustrate these changes with temperature, the spectra were deconvoluted into Lorentzian-shaped peaks. Four representative fitted peaks for (a) ZFH (150 K), (b) ZFH (390 K), (c) ZFH (800 K), and (d) ZFC (150 K) are shown in Fig. 3. Comparison between Figs. 3(a) and 3(b) suggests that three distinct variations occurred at 390 K: (1) a new Raman active mode appeared near 200 cm^{-1}; (2) the peaks centered at 135 and 526 cm^{-1} became broader; (3) the intensity of Raman modes at 249, 315, and 618 cm^{-1} changed evidently. It should be noted that this temperature (390 K) corresponded to the onset of dielectric dispersion around T_d, where the piezoelectric properties drastically degenerate.

The existence of nonpolar or antiferroelectric phases in NBT-BT materials has previously been proposed to account for the depolarization and relaxor behavior of these materials near T_d.[6,10] These proposed phases were identified to have *T* (*P*4bm) symmetry with antiparallel displacement of the Na^{1+}/Bi^{3+} and Ti^{4+} cations in the unit cell.[10] Our Raman data are consistent with this viewpoint. Based on group theory analysis,[16] there are 15 Raman-active modes for the antiferroelectric *T* (*P*4bm) phase: $\Gamma_{Raman} = 3A_1 + 3B_1 + 2B_2 + 7E$, whereas 8 Raman-active modes are predicted for the ferroelectric *T* (*P*4mm) phase: $\Gamma_{Raman} = 3A_1 + B_1 + 4E$. Thus, the new Raman mode (~200 cm^{-1}) detected at T_d may reveal a change in symmetry to a phase with a higher number of Raman active modes, although it is difficult to identify all the bands of the *T* (*P*4bm) phase. However, this particular mode was also observed for the $(Na_{1/2}Bi_{1/2})TiO_3$-$(K_{1/2}Bi_{1/2})TiO_3$ system,[17] where the unexpected appearance of the peak at ~200 cm^{-1} was considered to indicate the presence of the *T* (*P*4bm) phase. Thus, it is reasonable to suggest that the present samples underwent phase transition from ferroelectric *T* (*P*4mm) to antiferroelectric *T* (*P*4bm) phase. Furthermore, the anomalous changes in band frequency, width, and mode intensity close to T_d further support the occurrence of this transition.

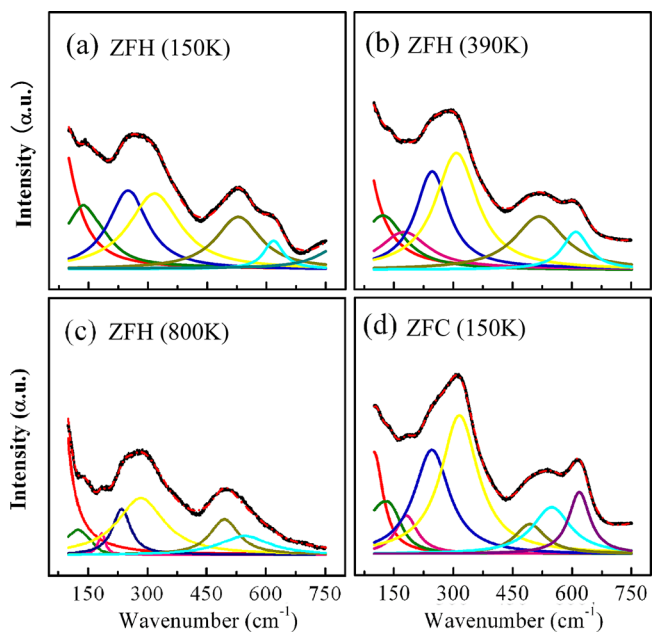

FIG. 3. Raman spectra deconvolution for [001]-poled Mn:NBT-5.0%BT crystal during ZFH and ZHC condition: (a) ZFH(150 K), (b) ZFH(390 K), (c) ZFH(800 K), and (d) ZFC(150 K).

Figure 3(c) shows the Raman spectrum of the high temperature (800 K) cubic phase. This spectrum is contradictory with the group theory, as none of modes for the ideal cubic (C) perovskite ABO_3 are Raman active.[12] However, in NBT-BT materials the random occupation at A-site sublattices of the perovskite unit cell by Bi^{3+}, Na^{1+}, and Ba^{2+} ions will cause the formation of polar nanoregions (or nanodomains). The presence of such nanoregions could result in a breakdown of the translation symmetry, causing the appearance of Raman bands for the cubic phase. Additionally, hot stage *in-situ* TEM on NBT-6.0%BT ceramics has revealed that the *P*4bm nanodomains evolve into the high temperature *C* phase.[10]

The Raman spectrum measured at 150 K under ZFC condition is shown in Fig. 3(d). The triple splitting of Raman modes (497, 554, and 618 cm^{-1}) in the TiO_6-octahedra vibration region was consistent with the presence of $a^-a^-a^-$ octahedral tilts in the *R* phase region.[14] Nevertheless, the presence of a double peak (249 and 315 cm^{-1}) with the additional mode at ~200 cm^{-1} agreed with the presence of $a^0a^0c^+$ octahedral tilts in the *T* phase region.[14] These phenomena can be better explained by two phase-coexistence

behavior. In other words, the high-temperature antiferroelectric *T* (*P*4bm) phase persisted into the *R* (*R*3c) phase field during the ZFC process, which was fortunately still visible in the micro-Raman. This was to be expected because the phase stability energies of the *T* (*P*4bm) phase are comparable to those of the *R* (*R*3c) phase near the MPB, allowing their coexistence in a wide temperature region.[6]

Figure 4 shows a summary of band frequency and intensity as a function of temperature for poled samples under ZFH and ZFC conditions. The appearance of the Raman mode at $\sim 200\,cm^{-1}$ clearly occurred at 390 K (Fig. 4(a)). The mode at $618\,cm^{-1}$ began to exhibit a steep change at 550 K and gradually merged into the mode at $526\,cm^{-1}$ at higher temperature. These observations for the ZFH condition suggested that the system underwent two phase transformations: from ferroelectric *T* to antiferroelectric *T* and from antiferroelectric *T* to paraelectric *C* at 390 and 550 K, respectively. In the ZFC condition [Fig. 4(b)], the mode at $526\,cm^{-1}$ split into a double mode (497 and $554\,cm^{-1}$), signifying a transition to the *R* phase at 375 K. The inconsistent ferroelectric transition temperature between ZFH (390 K) and ZFC (375 K) could be related to the nucleation of the relaxor/ferroelectric phase during heating/cooling, which was also found in a previous dielectric investigation.[8]

It has been recognized that the intensities of the Raman lines depend on the domain structure in the region where the laser beam is focused.[19] The intensity of the Ti–O modes (249 and $315\,cm^{-1}$) as a function of temperature is shown in Figs. 4(c) and 4(d). With the temperature increasing, the intensity of the Ti–O modes was almost constant, but an abrupt increase happens at $T_d \sim 390$ K (Fig. 4(c)). Thi *et al.* stated that the increasing intensity of the modes around $270\,cm^{-1}$ gives disorder information on the short-range arrangement of *A* cation-TiO_6 octahedra in lead-based relaxors.[22] Our temperature-dependent polarized light microscopy experiments also showed that *E*-field induced *T* ferroelectric macrodomains broke down at T_d. Therefore, the increase in the intensity of the Ti–O modes suggested that the induced long-range ordered macrodomains began to vanish, accompanied by the formation of a short-range ordered nanodomains. However, the Ti–O modes underwent hardening during the ZFC process ((Fig. 4(d)). This is apparently owing to an increment of the ferroelectric structural distortion, namely the *R* (*R*3c) polar nanoregions gradually nucleate and increase in volume fraction with decreasing temperature.

Since the octahedral vibrations and the Ti–O bonds are both influenced by the dynamics of the nanodomain phase,[19] the change in the octahedral modes (526 and $618\,cm^{-1}$) was also investigated as complementary to the Ti–O modes. Careful inspection of the Raman spectra measured at 375 and 390 K in Fig. 2(a) shows that the octahedral mode at $618\,cm^{-1}$ exhibited an abrupt increase in band intensity. This behavior is actually the same as that observed for the Ti–O modes (249 and $315\,cm^{-1}$), which have A_1 symmetry.[18,23] Meanwhile, the other octahedral mode at $526\,cm^{-1}$ underwent peak broadening because this mode possesses E symmetry.[24] These abrupt changes in the octahedral modes confirmed the phase transition around T_d, marking the beginning of the short-range ordered nanodomains. It should be noted that these results were also supported by our dielectric measurements.

In summary, [001]-oriented Mn:NBT-5.0%BT single crystals were systematically investigated by micro-Raman scattering. The evolution of the *E*-field induced Raman spectra revealed a field induced local distortions and *R*-*T* phase transition. Temperature-dependent Raman scattering performed on

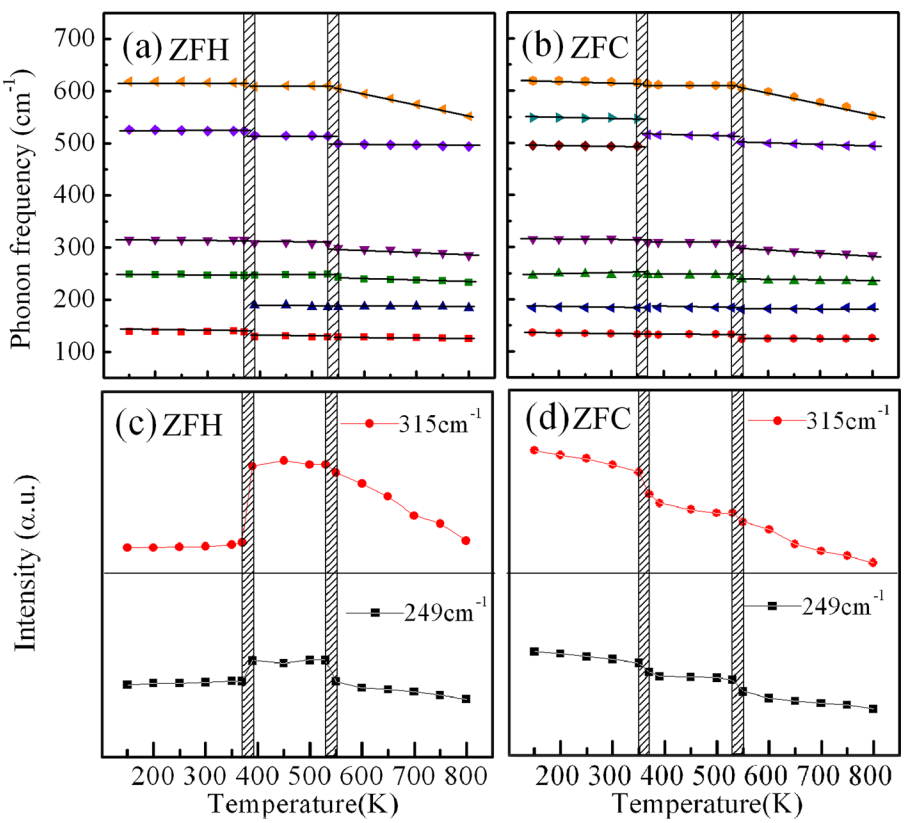

FIG. 4. The band frequency and intensity as a function of temperature: (a), (c) for ZFH and (b), (d) for ZFC, respectively.

poled samples in the range 150–800 K indicated that two phase transitions occurred with increasing temperature: from ferroelectric *T* to antiferroelectric *T* and from antiferroelectric *T* to paraelectric *C* at 390 and 550 K, respectively. The temperature dependences of the frequency shifts, peak numbers, and intensities of the Raman modes provided clear evidence of the sequence of these phase transitions.

This work was financially supported by the Ministry of Science and Technology of China through 973 Program (Nos. 2013CB632900 and 2009CB623305), the Natural Science Foundation of China (Nos. 61001041, 11090332, and 51272268), Science and Technology Commission of Shanghai Municipality (No. 12DZ0501000), Shanghai Rising-Star Program (No. 11QA1407500), Open Project from Shanghai Institute of Technical Physics, CAS (No. IIMDKFJJ-11-08), the Fund of Shanghai Institute of Ceramics (No. Y29ZC4140G), the CAS/SAFEA International Partnership Program for Creative Research Teams.

[1]T. Takenaka, K. Maruyama, and K. Sakata, Jpn. J. Appl. Phys., Part 1 **30**, 2236 (1991).
[2]W. Jo, J. E. Daniels, J. L. Jones, X. Tan, P. A. Thomas, D. Damjanovic, and J. Rödel, J. Appl. Phys. **109**, 014110 (2011).
[3]Q. H. Zhang, Y. Y. Zhang, F. F. Wang, Y. J. Wang, D. Lin, X. Y. Zhao, H. S. Luo, W. W. Ge, and D. Viehland, Appl. Phys. Lett. **95**, 102904 (2009).
[4]J. E. Daniels, W. Jo, J. Rödel, and J. L. Jones, Appl. Phys. Lett. **95**, 032904 (2009).
[5]W. W. Ge, C. T. Luo, Q. H. Zhang, C. P. Devreugd, Y. Ren, J. F. Li, H. S. Luo, and D. Viehland, J. Appl. Phys. **111**, 093508 (2012).
[6]W. Jo, S. Schaab, E. Sapper, L. A. Schmitt, H. J. Kleebe, A. J. Bell, and J. Rödel, J. Appl. Phys. **110**, 074106 (2011).
[7]C. Ma, H. Guo, S. P. Beckman, and X. Tan, Phys. Rev. Lett. **109**, 107602 (2012).
[8]F. Craciun, C. Galassi, and R. Birjega, J. Appl. Phys. **112**, 124106 (2012).
[9]H. Foronda, M. Deluca, E. Aksel, J. S. Forrester, and J. L. Jones, Mater. Lett. **115**, 132 (2014).
[10]C. Ma and X. Tan, J. Am. Ceram. Soc. **94**, 4040 (2011).
[11]W. Ge, H. Cao, C. DeVreugd, J. Li, D. Viehland, Q. Zhang, and H. Luo, J. Am. Ceram. Soc. **94**, 3084 (2011).
[12]M. Shen, G. G. Siu, Z. K. Xu, and W. Cao, Appl. Phys. Lett. **86**, 252903 (2005).
[13]J. Kreisel, A. Glazer, P. Bouvier, and G. Lucazeau, Phys. Rev. B **63**, 174106 (2001).
[14]L. Luo, W. Ge, J. Li, D. Viehland, C. Farley, R. Bodnar, Q. Zhang, and H. Luo, J. Appl. Phys. **109**, 113507 (2011).
[15]B. Wylie-van Eerd, D. Damjanovic, N. Klein, N. Setter, and J. Trodahl, Phys. Rev. B **82**, 104112 (2010).
[16]D. Rout, K. S. Moon, S. J. L. Kang, and I. W. Kim, J. Appl. Phys. **108**, 084102 (2010).
[17]J. Kreisel, A. M. Glazer, G. Jones, P. A. Thomas, L. Abello, and G. Lucazeau, J. Phys.: Condens. Matter **12**, 3267 (2000).
[18]D. Rout, K. S. Moon, V. S. Rao, and S. J. L. Kang, J. Ceram. Soc. Jpn. **117**, 797 (2009).
[19]A. Slodczyk, P. Colomban, and M. Pham-Thi, J. Phys. Chem. Solids **69**, 2503 (2008).
[20]S. Gupta, R. S. Katiyar, R. Guo, and A. S. Bhalla, J. Raman Spectrosc. **31**, 921 (2000).
[21]W. W. Ge, J. J. Yao, C. DeVreugd, J. F. Li, D. Viehland, Q. H. Zhang, and H. S. Luo, Solid State Commun. **151**, 71 (2011).
[22]M. P. Thi, G. March, and P. Colomban, J. Eur. Ceram. Soc. **25**, 3335 (2005).
[23]I. Gregora, P. Ondrejkovic, E. Simon, M. Berta, M. Savinov, J. Hlinka, H. Luo, and Q. Zhang, Ferroelectrics **404**, 220 (2010).
[24]D. Schütz, M. Deluca, W. Krauss, A. Feteira, T. Jackson, and K. Reichmann, Adv. Funct. Mater. **22**, 2285 (2012).